Patient-Derived Intrafemoral Orthotopic Xenografts of Peripheral Blood or Bone Marrow from Acute Myeloid and Acute Lymphoblastic Leukemia Patients: Clinical Characterization, Methodology, and Validation

Lintao Bi (bilt@jlu.edu.cn)
Jilin University
Jun Li
Jilin University
Hongkui Chen
Shanghai LIDE Biotech, Co. Ltd
ShiZhu Zhao
Shanghai LIDE Biotech, Co. Ltd
Danyi Wen
Shanghai LIDE Biotech, Co. Ltd

Research Article

Keywords: acute leukemia, patient-derived orthotopic xenograft (PDOX), methodology, peripheral blood, bone marrow

Posted Date: March 16th, 2022

DOI: https://doi.org/10.21203/rs.3.rs-1444342/v1

Abstract

Acute myeloid leukemia (AML) and acute lymphoblastic leukemia (ALL) are malignant clonal diseases of the hematopoietic system with an unsatisfactory overall prognosis. The main obstacle is the increased resistance of AML and ALL cells to chemotherapy. The development and validation of new therapeutic strategies for acute leukemia require preclinical models that accurately recapitulate the genetic, pathological, and clinical features of acute leukemia. A patient-derived xenograft (PDX) model is established by transplanting patient tumor tissue or cells into immunocompromised or humanized mice. They closely resemble human tumor progression and microenvironment and are more reliable translational research tools than other models. A patient-derived orthotopic xenograft (PDOX) model that transplants tumor cells into the corresponding anatomical site in mice better recapitulates human tumor behavior than subcutaneous or intravenous xenografts. In this study, we established bone marrow and peripheral blood cell models of AML and ALL patients, characterized their pathology, cytology, and genetics, and compared the model's characteristics and drug responsiveness with those of the corresponding patients.

Introduction

Leukemia is a common malignancy worldwide. Acute myeloid leukemia (AML) and acute lymphoblastic leukemia (ALL) are monoclonal neoplastic proliferations of myeloid precursors or lymphoid progenitor cells. Ongoing advances in treatment have significantly improved 5-year survival, but the overall prognosis of acute leukemia is not satisfactory (1). About 50% of AML patients and 20% of ALL patients experience a relapse, which is the greatest challenge in the management of acute leukemia (2,3). The main obstacle in the treatment of acute leukemia is the increased resistance of AML and ALL cells to chemotherapy (4, 5). The development and validation of novel therapeutic strategies for acute leukemia require preclinical models that accurately recapitulate the genetic, pathological, and clinical characteristics of AML and ALL.

Preclinical experimental models of acute leukemia are limited because they differ from human disease in genetic heterogeneity, pathological characteristics, and drug responsiveness (6). Patient-derived xenograft (PDX) models are established by transplantation of patient tumor tissue or cells into immunocompromised mice. They are reliable tools for translational research than other models (7). PDX models using immunodeficient mice are limited by the lack of interaction between tumor cells and immune cells. Patient-derived orthotopic xenograft (PDOX) models, with implantation of tumor cells into the corresponding anatomical position in mice, better recapitulate human tumor behavior than subcutaneous or intravenous xenografts [8]. As PDOX models mimic the drug sensitivity of the corresponding patient, they potentially benefit personalized therapy of acute leukemia [9].

This study investigated the usefulness of PDOX mouse models of AML and ALL for the study of drug sensitivity and resistance. We established models from patients with AML and ALL, characterized their pathological, cytological, and genetic features, and compared the features and drug responsiveness of the models with those of the corresponding patients.

Materials And Methods

AML and ALL *patient samples*

Peripheral blood or bone marrow samples were obtained from AML and ALL patients at the China–Japan Union Hospital of Jilin University. The study was reviewed and approved by the Institutional Ethics Committee, and written informed consent for study enrollment and blood or bone marrow collections was obtained from all patients.

Antibodies and other reagents

Antibodies (Abs) used for flow cytometry, PE mouse antihuman CD33 (Cat#: 555450) and APC mouse antihuman CD45 (Cat#: 555485) were purchased from BD Biosciences, PerCP/Cy5.5 antihuman CD19 (Cat#: 302229) was purchased from Biolegend. Cytarabine (Cat#: BD8499), imatinib (Cat#: BD42606), and ibrutinib (Cat#:BD254580) were purchased from Bide Pharmatech (Shanghai, China). Epirubicin (Cat#: 56390-09-1) was purchased from Shandong New Time Pharmaceutical Co., Ltd., Company (Shandong, China). Vincristine (Cat#: MB1298) was purchased from Melone Pharma (Dalian, China). Cladribine (Cat#:CSN10004) was purchased from CSNpharma (Shanghai, China).

Animals

The immunodeficient NCG (NOD/ShiLtJ-Prkdc em26Cd52 Il2rg em26Cd22) mice used in this study were purchased from GemPharmatech Co., Ltd. Company (Nanjing, China) and maintained in pathogen-free conditions at Shanghai LIDE Biotechnology Co., Ltd., Company (Shanghai, China).

Establishment of the PDOX models using peripheral blood or bone marrow

6- to 8-week-old NCG mice were were injected intrafemorally with $1–2\times10^6$ peripheral blood or bone marrow cells of AML or ALL patients after being anesthetized with a 1.25% avertin solution, respectively.

Evaluation of the PDOX models and patient samples

Flow cytometry: Engraftment of the orthotopic models was monitored by flow cytometry of peripheral blood from inoculated mice. The frequencies of $CD45^+CD33^+$ expression in AML and $CD45^+CD19^+$ expression for B-ALL were assayed. A 5–15% dual positivity indicated AML or ALL PDOX engraftment. The procedures of PDOX establishment are shown in Figure 1. Staining and flow cytometry were performed following the manufacturers' protocols. An Attune NxT flow cytometer was used with Attune NxT v4.2.0 software.

Additional analysis:

The presence of gene mutations that commonly occur in AML and ALL patients was investigated by next generation sequencing of peripheral blood and bone marrow samples obtained from the AML and B-ALL patients and the xenografts in the PDOX mouse spleen samples. Chromosomal analysis of human AML and ALL cells in mouse spleen samples from the established PDOX models was performed by karyotyping and standard G-banding.

Standard of care in AML and ALL PDOX models

Cladribine, cytarabine, imtatinib, or epirubicin in combination with vincristine were used to validate the in vivo efficacy of standard chemotherapies in the AML and ALL PDOX models. Cladribine and imatinib was given daily via gavage at 0.4 mg/dose and 25 mg/kg, respectively. Cytarabine was given on days 1–5 by intraperitoneal injection at 10 mg/kg. Epirubicin was given weekly by intraperitoneal injection at 1 or 2.5 mg/kg. Vincristine was given weekly by intravenous injection at 0.5 mg/kg. The body weight of each animal was recorded every day, and doses were normalized against the individual weight to ensure consistency among groups. Flow cytometry was performed weekly to determine AML/ALL progression and the antitumor effectiveness of each treatment.

Results

Identification of patient samples

In the validation phase, we identified potential markers and targets in patient samples by next generation sequencing, G-banding, and flow cytometry, and the results are shown in Table I.

Tab. I

Cell surface markers, chromosome characteristics, and genetic analysis in patients

Model ID	FACS analysis	Chromosomal analysis	Gene mutation
LD1-0040-361280	CD33+MPO+	No	NPM1exon12A+
LD1-0040-362349	CD34+CD117+CD13+CD33+CD38+	t(9;11)(p22;q23)[10]	WT1exon7,c.1107A>G TP53exon4,c.215C>G ASXL1exon13,c.3759T>C ASXL1_3'UTR,c.*22A>G TET2exon3,c.86C>G DNMT3Aexon2,c.27C>T DNMT3Aexon9,c.1122+7G>A DNMT3Aexon10,c.1266G>A DNMT3Aexon18,c.2173+26C>T DNMT3Aexon22,c.2597+30G>A MLL AF9 fusion
LD1-0040-362384	HLA-DR+CD13+CD15+CD33+MPO+	-2, add(3)(p21), add(4)(q31), del(6)(q21q23), i(17)(q10), +mar[2]/45, sl, -10[5]/46, sdl, +18[3]	ND
LD1-0040-362030	CD38+CD33+CD123+MPO+	Normal	ND
LD1-0040-361780	CD13+CD33+CD56+MPO+CD117+	Normal	FLT3 ITD>93bp insertion NPM1A+ DNMT3Aexon9,c.1122+7G>A DNMT3Aexon18,c.2173+26C>T DNMT3Aexon22,c.2597+30G>A TET2exon6,c.3647G>C TET2exon6,c.3653C>G TET2exon11,c.5162T>G ASXL1exon12,c.3759T>C ASXL1 3'UTR,c.*22A>G TP53exon2,c.74+14T>C TP53exon4,c.97 29C>A TP53exon4,c.215C>G
LD1-0040-362224	CD13+CD123+MPO+CD33dimCD34dimCD64dimCD117dim	ND	HOX11+ FLT3 ITD>21bp insertion NPM1A+ DNMT3Aexon9,c.1122+7G>A DNMT3Aexon10,c.1266G>A TET2exon3,c.86C>G TET2exon3,c.2474delC TET2exon11,c.5082_5083insA ASXL1exon13,c.3758T>C ASXL1 3'UTR,c.*22A>G WT1exon7,c.1107A>G TP53exon4,c.97 29C>A
LD1-0040-362369	CD34+CD117+CD33+CD13+CD38+	t(7;11)(p15;p15)[10]	DNMT3Aexon9,c.1122+7G>A DNMT3Aexon10,c.1266G>A DNMT3Aexon18,c.2173+26C>T DNMT3Aexon22,c.2597+30G>A DNMT3Aexon23,c.2674T>A TET2exon11,c.5284A>G ASXL1exon13,c.3759T>C ASXL1 3'UTR,c.*22A>G WT1exon7,c.1107A>G
LD1-0040-362393	CD33+CD38+MPO+	Normal	HOX11+ NPM1A+ DNMT3Aexon2,c.27C>T DNMT3Aexon9,c.1122+7G>A DNMT3Aexon10,c.1266G>A DNMT3Aexon18,c.2173+26C>T DNMT3Aexon22,c.2597+30G>A DNMT3Aexon23,c.2645G>A TET2exon3,c.3253_3256delA CAA TET2exon6,c.3743T>A TET2exon11,c.5284A>G TET2exon11,c.5412T>C WT1exon7,c.1107A>G TP53exon4,c.215C>G KRAS exon2,c.38G>A SRSF2exon1,c.284C>A TET2exon11,c.5540G>A NPM1exon11,c.860_863dupTCTG
LD1-0040-362499	CD117+CD33+CD123+CD56dimCD38+CD33+CD15+CD64+HLA-DR+CD36+CD11bdimCD13dimCD14dimCD9dim	Normal	
LD1-0040-362575	CD34+CD33+CD13+MPO+CD9+CD4dimCD11bdimHLA-DR+CD11c+CD38+CD14+CD123+CD64+CD2+CD36+	Normal	KITexon8,c.1251_1257>GGGA
LD1-0041-362073	CD34+HLA-DR+CD33+CD123+CD9+CD19+CD10+cCD79a+TDT+CD13+CD22+	+5, t(9;22), +der(22)t(9;22)	EP300exon6>p.S507G
LD1-0041-362356	CD45dimCD10+cCD22+CD19+CD33+	ND	JAK2exon16>p.R683S
LD1-0041-362478	CD45dimCD19+CD10+CD34+HLA-DR+CD9+CD24+CD58+CD38+cκdim	Normal	ND
LD1-1041-362519	CD38+HLA-DR+CD22+CD19+CD10+CD9+cCD79a+	del(1q), add(9p), del(9p), der(9), del(18q)	BRINP3exon7>p.A369V CREBBPexon2>p.A254T MED12exon8>p.A412T
LD1-0041-362021	CD19+CD22+CD34+CD38+cCD79a+	del(9)(p21)[20]	ND

Engraftment of AML and ALL PDOX model evaluated by fluorescence-activated cell sorting (FACS)

Patient characteristics, diagnosis, and treatment history, are shown in Table II. Xenograft models of AML and ALL were prepared by intrafemoral injection of fresh blasts from the peripheral blood (PB) or bone marrow (BM) of leukemia patients into NCG mice and screened for their potential to initiate leukemia in the mouse models. The frequency of $CD45^+CD33^+$ cells or $CD45^+$ cells in mouse peripheral blood was monitored weekly by FACS beginning 3–4 weeks after transplantation. To confirm the engraftment of human AML/ALL in the mouse models. P0 indicates the primary passage of patient cell suspension prepared from patient blood or bone marrow samples. When the percentage of positive cells reached 10%, single cell suspensions prepared from the mouse spleen were inoculated intrafemorally into naïve NCG mice (P1), or cryopreserved in liquid nitrogen until inoculation (FP0+1). The percentages of leukemia cells at P0, P1, and FP0+1 in 12 representative PDOX models are shown in Figure 2. Successfully engraftment of PDOX models was defined as 10% $CD45^+CD33^+$ or $CD45^+$ at P1. Successfully established PDOX required stable morphologic and molecular characteristics for at least two passages.

Tab. II

Patient characterization

Summarized clinical data of patients at the time of sample withdrawal. All samples used in this study were from patients with AML/ALL.

	Model ID	Sex	Age	Sample	Clinical diagnosis	Treatment history (sequentially)
AML	LD1-0040-361280	Female	38	Bone Marrow	AML	Idarubicin+Cytarabine Cytarabine+Cladribine
	LD1-0040-362349	Male	23	Bone Marrow	AML metastatic seminoma	Idarubicin+Cytarabine High-dose Cytarabine
	LD1-0040-362384	Male	59	peripheral blood	New-diagnosed AML	Azacitidine+Homoharringtonine+Cytarabine Idarubicin+Cytarabine
	LD1-0040-362030	Female	56	peripheral blood	New-diagnosed AML	Idarubicin+Cytarabine High-dose Cytarabine Homoharringtonine+Cytarabine Chidamide Anti-PD-1 ab
	LD1-0040-361780	Male	49	peripheral blood	New-diagnosed AML	Idarubicin+Cytarabine High-dose Cytarabine Azacitidine+Homoharringtonine+Cytarabine Azacitidine+Chidamide Etoposide+Cytarabine
	LD1-0040-362224	Male	75	Bone Marrow	New-diagnosed AML	Hydroxycarbamide
	LD1-0040-362369	Male	57	Bone Marrow	New-diagnosed AML	Idarubicin+Cytarabine High-dose Cytarabine Azacitidine
	LD1-0040-362393	Female	57	peripheral blood	New-diagnosed AML	Idarubicin+Cytarabine Idarubicin+High-dose Cytarabine Cytarabine+Azacitidine+Homoharringtonine
	LD1-0040-362499	Male	68	peripheral blood	New-diagnosed AML	N/A
	LD1-0040-362575	Female	31	Bone Marrow	New-diagnosed AML	Idarubicin+Cytarabine High-dose Cytarabine
ALL	LD1-0041-362073	Male	64	Bone Marrow	Recurrent ALL	CVDP Imatinib Cytarabine
	LD1-0041-362356	Male	53	Bone Marrow	B-ALL	N/A
	LD1-0041-362478	Male	15	Bone Marrow	ALL	CVDLP Cytarabine MTX
	LD1-1041-362519	Female	38	Bone Marrow	Recurrent ALL	CVDLP Ibrutinib
	LD1-0041-362021	Male	32	Bone Marrow	New-diagnosed ALL	N/A

Cell suspensions prepared from patient samples were injected intrafemorally into NCG mice to generate the PDOX models. The frequency and percentage of CD45+ or CD45+CD33+ cells in mouse peripheral blood were determined by FACS at P0 (black lines), P1 (red lines), and FP0+1 (blue lines) of established PDOX models. Individual mice are shown as point values. Group results are shown with bars that give the standard deviation.

Cell suspensions prepared from patient samples were injected intrafemorally into NCG mice to generate the PDOX models. The frequency and percentage of $CD45^+$ or $CD45^+CD33^+$ cells in mouse peripheral blood were determined by FACS at P0 (black lines), P1 (red lines), and FP0+1 (blue lines) of established PDOX models. Individual mice are shown as point values. Group results are shown with bars that give the standard deviation.

Consistency of cell surface markers in patient samples and PDOX models

FACS analysis of cell surface markers in peripheral blood of patient samples and the PDOX models established using the samples are shown in Table III. CD19 was positive in both patient samples and all four of the corresponding PDOX ALL models. The ALL were B cell-derived phenotypes. All four were $CD10^+$ and $CD38^+$, suggesting that $CD19^+CD10^+CD38^+$ cell populations might be a useful as a panel to determine the establishment of PDOX in this type of B-ALL. The series of ALL-associated antigens revealed that the immunophenotype of PDOX cells was consistent with the primary specimens for most antigens tested and that they preserved the disease characteristics of the patients that they originated from.

Tab. III

Consistency of partial PDOX with the clinical: FACS analysis

Model ID	Clinical		PDOX FACS	
	Immunophenotype	Result	Immunophenotype	Result
LD1-0041-362073	abnormal cells	69.44%	abnormal cells	86.77%
	CD34	+	CD34	+
	HLA-DR	+	HLA-DR	No detection
	CD33	+	CD33	No detection
	CD123	+	CD123	+
	CD9	+	CD9	No detection
	CD19	+	CD19	+
	CD10	+	CD10	+
	cCD79a	+	cCD79a	No detection
	TDT	+	TDT	+
	CD13	+	CD13	No detection
	CD22	+	CD22	No detection
			CD24	+
			CD81dim	+
			CD73	+
	CD20	-	CD20	-
	CD38	-	CD38	-
LD1-1041-362519	abnormal cells	90.83%	abnormal cells	94.74%
	CD38	+	CD38	+
	HLA-DR	+	HLA-DR	No detection
	CD22	+	CD22	No detection
	CD19	+	CD19	+
	CD10	+	CD10	+
	CD9	+	CD9	No detection
	cCD79a	+	cCD79a	No detection
	CD34	+/-	CD34	-
	TDT	+/-	TDT	No detection
			CD81	+
	CD20	-	CD20	-
	CD123	-	CD123	-
LD1-0041-362021	abnormal cells	94.40%	abnormal cells	80.25%
	CD19	+	CD19	+
	CD22	+	CD22	No detection
	CD34	+	CD34	+
	CD38	+	CD38	+
	cCD79a	+	cCD79a	No detection
	CD10	-	CD10dim	+
	cIgM	-	cIgM	No detection
			CD24	+

			CD81dim	+
			CD123	+
	CD20	-	CD20	-
			CD73	-
LD1-0041-362478	abnormal cells	84.98%	abnormal cells	98.44%
	CD19	+	CD19	+
	CD10	+	CD10	+
	CD34	+	CD34	-
	HLA-DR	+	HLA-DR	No detection
	CD9	+	CD9	No detection
	CD24	+	CD24	No detection
	CD58	+	CD58	No detection
	CD38	+	CD38	+
	cκdim	+	cκdim	No detection
			CD81	+
			CD20	-
			CD123	-

Note:"+" means positive, "-" means negative.

Chromosome analysis of clinical samples and PDOX cells

G-banding karyotype analysis showed normal karyotypes and revealed that the karyotype of PDX cells was similar to that of patient specimens. (Table IV, Figure 3)

Tab. IV

Consistency of partial PDX/PDOX with the clinical: Chromosomal analysis

Model ID	Tissue type	Clinical result	PDOX result
LD1-0041-362073	peripheral blood	+5	
		t(9;22)(q34;q11.2)[18]/51	t(9;22)(q34;q11.2)
		+der(22)t(9;22)(q34;q11.2)[1]/48	der(22)t(9;22)[cp14]/46
LD1-1041-362519	Bone marrow	del(9)(p13)	Normalization
		der(9)[18]/46	-9
		add(9)(p13)	del(9)(p22)
		del(1)(q21)	Normalization
		del(18)(q21)	Normalization
LD1-0041-362021	Bone marrow	Normalization	Normalization
		Normalization	del(9)(p12p21)
		del(9)(p21)[20]	i(17)(q10)[20]

PDOX and the parental clinical sample have similar genetic profiles

An AML patient (LD1-0040-361280) had a mutation on exon 12 of NPM1, a typical hot-spot alteration seen in AML patients without chromosome abnormalities [13]. As shown in Table V, an NPM1exon12A mutation was found in the PDOX model by either RNAseq or whole exon sequencing.

Other mutations such as c-kit/D816V, CEBPA, or FLT3/ITD that are often found in AML were not present in either the PDOX model or the original patient sample. The result indicates consistency in the genetic profiles of the patient and the PDOX model.

Tab. V

Consistency of partial PDX/PDOX with the clinical: Genetic alteration

Model ID	Gene	Clinical result	PDOX result				
			WES_Mut(AF)	RNA_Mut(AF)	RNA_TPM	RNA_TPM_zscore_GTEx	RNA_TPM_zscore_TCGA
LD1-0040-361280	c-kit/D816V	-	-	-	12.5	4.200862	-1.08643
	CEBPA	-	-	-	117.22	1.922675	0.460406
	NPM1exon12A	+	Trp288fs(0.312)	Trp288fs(0.355)	1558.02	4.793047	3.388323
	FLT3/ITD	-	-	-	146.78	2.790451	0.758332

Standard of care validation with therapeutic regimens used in clinical practice

Validation using the same treatments that were administered to patient was performed in five of the established PDOXs. Cytarabine, which is commonly given to AML/ALL, patents had antitumor activity in both the AML and the ALL PDOXs (Figure 4B–E). In the AML PDOX, cladribine completely eliminated the tumor (Figure 4A). Epirubicin and vincristine, which are components in CEOP treatment [14] had good anti-tumor activity in three of the four ALL PDOX models (Figure 4C–E), but not in the LD1-0040-362519 model (Figure 4F). Imatinib and ibrutinib, two small molecules that target BCR-Abl and BTK, respectively, were not effective in all the PDOX models (Figure 4C and F). As shown in Table II, response or nonresponse of the PDOX models was consistent with the clinical outcomes that occurred in response to those agents by the corresponding patients. The patient responses to treatment were maintained in the PDOX mouse models.

Discussion

AML and ALL PDOX mouse models were established by intrafemoral injection of leukemia cells from patients into triple immunodeficient NCG mice. The xenografted mouse models faithfully mimicked the pathology, cytology, karyotype, and genetic profile of the corresponding patient samples. The responsiveness of the AML and ALL PDOX mouse models to chemotherapy drugs was highly consistent with the clinical outcomes of the corresponding patients. The findings suggest that the AML and ALL PDOX mouse models established in this study preserved the features of the disease in the patients.

Heterogeneity of the malignant cells, with multiple mutant clones and subclones is a hallmark of acute leukemia [10, 11]. Tumor cell heterogeneity in acute leukemia reduces the effectiveness of treatment [12]. Culturing and passaging exert a selective pressure on leukemia cells that favors the survival of undifferentiated cells and results in loss of original tumor cell heterogeneity [13]. Therefore, the behavior of leukemia cell lines is profoundly different from the patient's original tumor. PDX models of AML and ALL, which better represent the genetic and phenotypic heterogeneity of the corresponding leukemia, are indispensable for translational studies in acute leukemia [14, 15]. Establishment of PDX models of hematological malignancies remains challenging because leukemia cells have low take rate when transplanted into mice. The low success rate might be the result residual natural killer (NK) cell activity in nonobese diabetic (NOD)/severe combined immunodeficient (SCID) mice [9, 16, 17]. Crossbreeding NOD/SCID and interleukin (IL)-2 receptor γ-deficient mice has produced triple immunodeficient NCG, NSG, or NOG mice that lack functional T, B, and NK cells and are available from a number of suppliers [18]. The use of the triple immunodeficient NSG and NOG mouse models has significantly improved the efficiency of ALL and AML tumor engraftment in mouse models [19–21]. Triple immunodeficient NCG mice are not yet widely used to generate PDX models. This study demonstrated that NCG mice are an ideal model for the establishment of AML and ALL PDX models.

The implantation site of cancer cells affects the growth characteristics and phenotype of the PDX model [22]. Early PDX models of leukemia were established by heterotopically implanting cancer cells into the subcutaneous or intravenous space [8–10], and patient-derived heterotopic xenografts are widely used in cancer research. In this study, leukemia cells were injected intrafemorally into NCG mice to generate PDOXs. It is technically easier to perform and monitor tumor size of heterotopic implantation than establishing PDOXs [15]. Establishment of the leukemia PDOX model is time-consuming and technically challenging. The main advantage of PDOX models is a preserved tumor microenvironment and better modeling of tumor metastasis than heterotopic implantation [11].

An ideal research model should recapitulate the phenotypic and genetic characteristics of the original tumor in patients. In this study, the pathology of the mouse spleen and the surface markers of the engrafted cells from the PDOX models faithfully resembled the phenotypes of the patient leukemia samples. The karyotypes of PDOX cells were also highly consistent with those of the patient samples. We also compared the genetic profiles of PDOX models, and the clinical samples used for grafting by next generation sequencing. The *NPM1* gene is the most frequently mutated gene in

AML. We found that the *NPM1* gene mutation in the PDOX model was consistent with the patient's bone marrow sample, suggesting the PDOX model has stable genetic profiling.

In conclusion, it is feasible to establish AML and ALL PDOX models using the triple immunodeficient NCG mouse model. The established PDOX models preserve the pathological, phenotypic, and genetic characteristics of the clinical samples, and they also have similar drug sensitivity to the corresponding patients. The PDOX mouse model of acute leukemia provides a clinically relevant platform for testing novel chemotherapy drugs. Ultimately, the PDOX mouse model may be used for developing precision medicine approaches to treat leukemia.

Declarations

Acknowledgment

We are grateful to Yanbin Zhou, Zheng Yang, and Shuai Wang for their contributions to the success of the study.

Authors' contributions

Lintao Bi and Danyi Wen designed this study. Jun Li, Hongkui Chen and ShiZhu Zhao, performed experiments. Lintao Bi , Danyi Wen, Jun Li, Hongkui Chen and ShiZhu Zhao

analyzed the data in this paper. Jun Li and Hongkui Chen wrote the manuscript. Lintao Bi and Danyi Wen revised the manuscript. Lintao Bi and Danyi Wen reviewed and supervised

the experiments. All authors read and approved the final manuscript.

Declaration of Conflicting Interests

The author(s) declared no potential conflicts of interest with respect to the research, authorship, and/or publication of this article.

References

1. H.M. Kantarjian, T.M. Kadia, C.D. DiNardo, M.A. Welch, F. Ravandi, Acute myeloid leukemia: Treatment and research outlook for 2021 and the MD Anderson approach, Cancer 127(8) (2021) 1186-1207.
2. F. Thol, A. Ganser, Treatment of Relapsed Acute Myeloid Leukemia, Curr Treat Options Oncol 21(8) (2020) 66.
3. B. Samra, E. Jabbour, F. Ravandi, H. Kantarjian, N.J. Short, Evolving therapy of adult acute lymphoblastic leukemia: state-of-the-art treatment and future directions, J Hematol Oncol 13(1) (2020) 70.
4. J. Zhang, Y. Gu, B. Chen, Mechanisms of drug resistance in acute myeloid leukemia, Onco Targets Ther 12 (2019) 1937-1945.
5. H. Kantarjian, T. Kadia, C. DiNardo, N. Daver, G. Borthakur, E. Jabbour, G. Garcia-Manero, M. Konopleva, F. Ravandi, Acute myeloid leukemia: current progress and future directions, Blood Cancer J 11(2) (2021) 41.
6. H. Sajjad, S. Imtiaz, T. Noor, Y.H. Siddiqui, A. Sajjad, M. Zia, Cancer models in preclinical research: A chronicle review of advancement in effective cancer research, Animal Model Exp Med 4(2) (2021) 87-103.
7. D. Sia, A. Moeini, I. Labgaa, A. Villanueva, The future of patient-derived tumor xenografts in cancer treatment, Pharmacogenomics 16(14) (2015) 1671-83.
8. R.M. Hoffman, Patient-derived orthotopic xenografts: better mimic of metastasis than subcutaneous xenografts, Nat Rev Cancer 15(8) (2015) 451-2.
9. J. Bhimani, K. Ball, J. Stebbing, Patient-derived xenograft models-the future of personalised cancer treatment, Br J Cancer 122(5) (2020) 601-602.
10. S. Horibata, G. Gui, J. Lack, C.B. DeStefano, M.M. Gottesman, C.S. Hourigan, Heterogeneity in refractory acute myeloid leukemia, Proc Natl Acad Sci U S A 116(21) (2019) 10494-10503.
11. C.E. Meacham, S.J. Morrison, Tumour heterogeneity and cancer cell plasticity, Nature 501(7467) (2013) 328-37.
12. Y. Lai, X. Wei, S. Lin, L. Qin, L. Cheng, P. Li, Current status and perspectives of patient-derived xenograft models in cancer research, J Hematol Oncol 10(1) (2017) 106.
13. M.E. Belderbos, T. Koster, B. Ausema, S. Jacobs, S. Sowdagar, E. Zwart, E. de Bont, G. de Haan, L.V. Bystrykh, Clonal selection and asymmetric distribution of human leukemia in murine xenografts revealed by cellular barcoding, Blood 129(24) (2017) 3210-3220.
14. E. Clappier, B. Gerby, F. Sigaux, M. Delord, F. Touzri, L. Hernandez, P. Ballerini, A. Baruchel, F. Pflumio, J. Soulier, Clonal selection in xenografted human T cell acute lymphoblastic leukemia recapitulates gain of malignancy at relapse, J Exp Med 208(4) (2011) 653-61.

15. M. Hidalgo, F. Amant, A.V. Biankin, E. Budinska, A.T. Byrne, C. Caldas, R.B. Clarke, S. de Jong, J. Jonkers, G.M. Maelandsmo, S. Roman-Roman, J. Seoane, L. Trusolino, A. Villanueva, Patient-derived xenograft models: an emerging platform for translational cancer research, Cancer Discov 4(9) (2014) 998-1013.
16. S. Okada, K. Vaeteewoottacharn, R. Kariya, Application of Highly Immunocompromised Mice for the Establishment of Patient-Derived Xenograft (PDX) Models, Cells 8(8) (2019).
17. R.B. Lock, N. Liem, M.L. Farnsworth, C.G. Milross, C. Xue, M. Tajbakhsh, M. Haber, M.D. Norris, G.M. Marshall, A.M. Rice, The nonobese diabetic/severe combined immunodeficient (NOD/SCID) mouse model of childhood acute lymphoblastic leukemia reveals intrinsic differences in biologic characteristics at diagnosis and relapse, Blood 99(11) (2002) 4100-8.
18. K.A. Lodhia, A.M. Hadley, P. Haluska, C.L. Scott, Prioritizing therapeutic targets using patient-derived xenograft models, Biochim Biophys Acta 1855(2) (2015) 223-34.
19. N. Hassan, J. Yang, J.Y. Wang, An Improved Protocol for Establishment of AML Patient-Derived Xenograft Models, STAR Protoc 1(3) (2020) 100156.
20. T. Tomii, T. Imamura, K. Tanaka, I. Kato, A. Mayumi, E. Soma, M. Yano, K. Sakamoto, T. Mikami, M. Morita, N. Kiyokawa, K. Horibe, S. Adachi, T. Nakahata, J. Takita, H. Hosoi, Leukemic cells expressing NCOR1-LYN are sensitive to dasatinib in vivo in a patient-derived xenograft mouse model, Leukemia 35(7) (2021) 2092-2096.
21. J.P. Loftus, A. Yahiaoui, P.A. Brown, L.M. Niswander, A. Bagashev, M. Wang, A. Schauf, S. Tannheimer, S.K. Tasian, Combinatorial efficacy of entospletinib and chemotherapy in patient-derived xenograft models of infant acute lymphoblastic leukemia, Haematologica 106(4) (2021) 1067-1078.
22. J. Schueler, G. Greve, D. Lenhard, M. Pantic, A. Edinger, E. Oswald, M. Lubbert, Impact of the Injection Site on Growth Characteristics, Phenotype and Sensitivity towards Cytarabine of Twenty Acute Leukaemia Patient-Derived Xenograft Models, Cancers (Basel) 12(5) (2020).

Figures

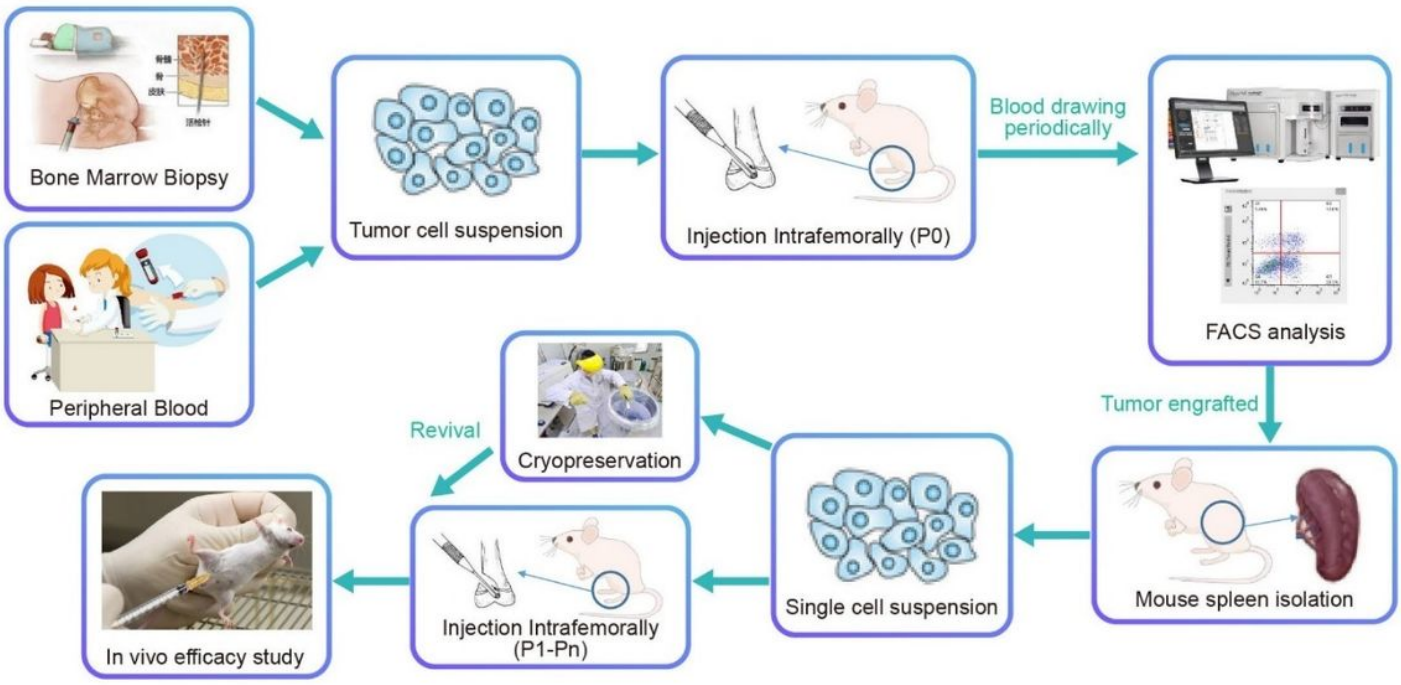

Figure 1

Procedures for PDOX establishment using AML/ALL samples.

Figure 2

Establishment of PDOX Model in NCG mice

Cell suspensions prepared from patient samples were injected intrafemorally into NCG mice to generate the PDOX models. The frequency and percentage of CD45+ or CD45+CD33+ cells in mouse peripheral blood were determined by FACS at P0 (black lines), P1 (red lines), and FP0+1 (blue

lines) of established PDOX models. Individual mice are shown as point values. Group results are shown with bars that give the standard deviation.

Figure 3

Karyotypes

(A) of peripheral blood from an ALL patient (model ID: LD1-0041-362073) and of (a) mouse peripheral blood from the LD1-0041-362073 PDOX model. (B) Karyotypes of bone marrow from an ALL patient (model ID: LD1-1041-362519) and of (b) mouse bone marrow from the LD1-1041-362519 PDOX model. (C) Karyotypes of bone marrow of an ALL patient (model ID: LD1-0041-362021) and (c) mouse bone marrow of the LD1-0041-362021 PDOX model

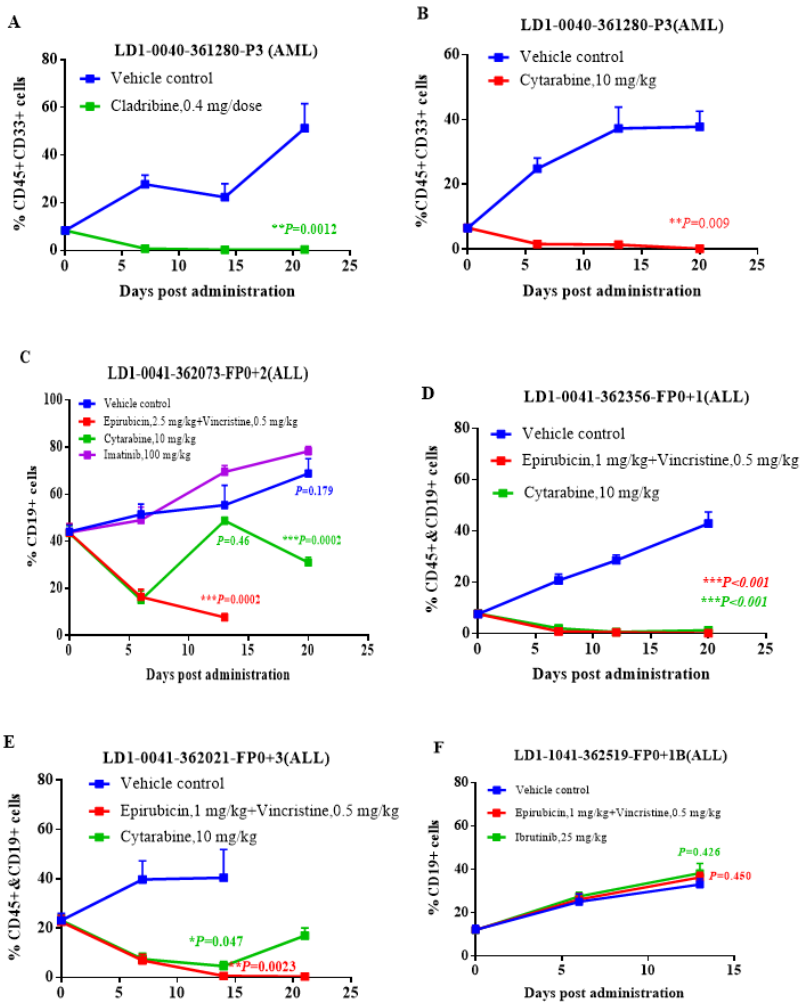

Figure 4

Standard of care validation in PDOX models.

AML PDOX (LD1-0040-361280) and ALL PDOXs (LD1-0040-362073, LD1-0040-362356, LD1-0040-362021, and LD1-0040-362519) models were used for standard of care validation. Treatment of the model mice began after randomization to the indicated regimen. Cell surface markers (CD45+, CD33+, and/or CD19+) were monitored weekly until the end of the study. Data are means ± standard deviation and $p < 0.05$ indicates statistical significance vs. control